CETRA2026 27-30 May 2026, Bol, Island Brač, Croatia
9th International Conference on Road and Rail Infrastructure

QUANTIFICATION AND ASSESSMENT OF SHORT-WAVE RAIL CORRUGATION

Gerald Riepl
Graz University of Technology, Institute of Railway Engineering and Transport Economics, Austria

Abstract

Short-wave corrugation on the rail surface, particularly on the inner rail in small-radius curves, arises from dynamic wheel–rail interactions and leads to increased maintenance demand, elevated acoustic emissions, and reduced ride comfort. This study investigates the temporal development of short-wave corrugation and the influence of curve radius and rail steel grade based on long-term rail surface measurement data from a heavily trafficked railway line with varying curve radii. Repeated measurements were processed into curve-specific time series and analyzed using linear regression to derive local corrugation growth rates for different radius classes ($R < 250$ m, $250 \text{ m} < R < 400$ m, and $400 \text{ m} < R < 600$ m) and rail steel grades (the standard grade R260 and the head-hardened grades R350HT and R400HT). The results show a strong dependence of corrugation growth on curve radius, with significantly higher growth rates in small-radius curves, identifying curvature as the dominant influencing factor. Rail steel grade has a secondary but measurable effect, with higher-strength rail steels generally exhibiting lower growth rates and reduced variability; the most favorable behavior is observed for R400HT. However, pronounced corrugation growth persists in small-radius curves even for heat-treated rail steels, indicating that material-related improvements alone cannot fully compensate for unfavorable geometric and loading conditions.

Keywords: short-wave rail corrugation, curve radius, rail surface measurement, corrugation growth rate, rail steel grade

1 Introduction

Rail corrugation has attracted scientific and engineering interest since the late nineteenth century and has been investigated and categorized in different forms of corrugation in terms of characteristics and treatments [1]. Despite the research history, rail corrugation remains a persistent problem in railway operation, associated with increased noise emission and degradation of track and vehicle components [2, 3]. Short-wave corrugation is characterized by periodic irregularities on the rail running surface that appear as a sequence of peaks and hollows [4]. The typical wavelength range is from 30 mm to 300 mm [4]. It occurs predominantly on the inner rail in curves and is marked by a highly even wavelength and appearance [5]. Corrugation amplitudes can develop rapidly to tenths of a millimeter, while discrete track irregularities such as welds or joints may act as initiation points and fix the longitudinal position of the corrugation [5]. From a mechanical perspective, corrugation develops when one wheel of a wheelset enters a sliding state while the opposite wheel would otherwise continue to roll, giving rise to a highly periodic stick–slip mechanism that activates a wavelength-fixing process [5]. Under practical operating conditions, deficient superelevation has been identified as a contributing factor to the occurrence and accelerated development of

DOI: https://doi.org/10.5592/CO/CETRA.2026.1955

short-wave corrugation in small-radius curves [6]. In particular, radii smaller than approximately 600 m are susceptible to short-wave corrugation on the inner rail [7]. In addition to geometric effects, the structural properties of the track system play a significant role in corrugation development [7]. Track with wooden sleepers, owing to its higher vertical elasticity, has been reported to mitigate dynamic corrugation-related deformations, whereas stiffer track structures, such as those with concrete sleepers, tend to promote the formation of short-wave corrugation [7]. Experimental investigations further indicate that contact conditions, such as wheel-rail interaction, influence corrugation development [8]. Forced corrugation experiments showed that corrugation formed under dry wheel–rail contact conditions, whereas no corrugation developed under lubricated conditions [8]. Building on the described mechanisms and influencing factors of short-wave rail corrugation, the present study focuses on quantifying its temporal development under real operating conditions.

2 Methodology

This section describes the methodological framework used to quantify the temporal development of short-wave rail corrugation based on long-term operational rail surface measurement data. The analysis focuses on a heavily trafficked railway line with a high proportion of small-radius curves, where corrugation-related damage occurs frequently. The evaluated curves are located within a continuous double-track mainline section without significant branching or traffic redistribution; therefore, comparable annual traffic loads can be assumed for all investigated curves. Relevant track sections were identified using a digital track database providing detailed geometric and infrastructure-related information for the investigated route. The evaluation concentrates on curved track segments with radii smaller than 600 m, as these sections are considered particularly susceptible to the formation and growth of short-wave corrugation. Track selection and structuring were performed for both tracks of the double-track line. For each selected curve, the corresponding mileage range and geometric parameters such as radius and curvature direction were compiled and used as a consistent structural reference for all subsequent analysis steps. For result presentation, curves were further classified into three radius classes ($R < 250$ m, $250 \text{ m} < R < 400$ m, and $400 \text{ m} < R < 600$ m), following the classification scheme of the underlying track database.
The analysis is based on repeated rail surface measurement runs conducted between 2012 and 2024. All measurement data are spatially referenced via the mileage data of the measurement vehicle, allowing signals from different runs to be consistently assigned to identical track segments. Prior to further processing, all datasets were subjected to plausibility checks, and incomplete, inconsistent, or non-comparable records were excluded. Rail steel grades documented in the infrastructure database were used to group results by material (R260, R350HT, and R400HT). While documented installation and renewal information was considered, the analysis relies on infrastructure records, which may contain uncertainties, particularly with respect to rail grade documentation. The methodological approach comprises the extraction and preprocessing of rail surface measurement signals for the selected curved track sections, followed by the construction of curve-specific time series describing the temporal evolution of rail surface condition. Based on these time series, regression-based evaluations are performed to quantify corrugation growth rates. The individual processing and evaluation steps are described in detail in the following subsections.

2.1 Rail surface measurement and signal processing

The rail surface measurement system has been in operational use on the Austrian railway network since 2005. It is based on three optical triangulation sensors aligned in the longitudinal rail direction, measuring the distance to the rail surface at the center of the rail head.

The front and rear sensors define a virtual chord, while the measured value corresponds to the vertical deviation of the rail surface relative to this chord, obtained from the central sensor [9]. Figure 1 illustrates the chord-based measurement principle. Depending on the local rail surface geometry, the measured chord value may be positive or negative, as the rail surface can locally lie above or below the virtual chord.

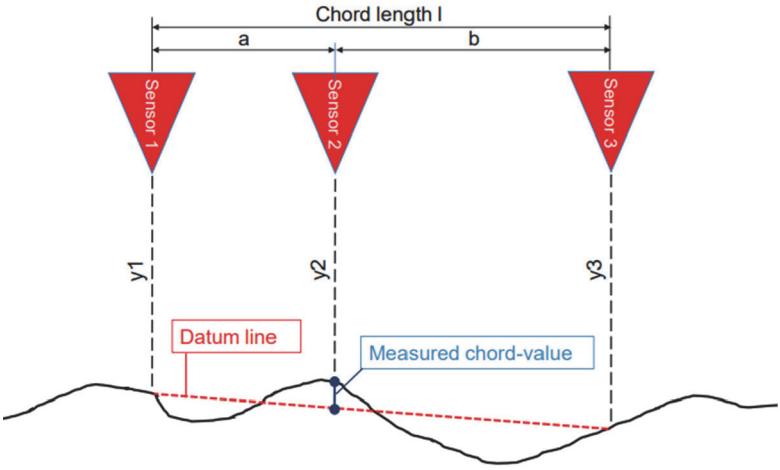

Figure 1 Chord-based measurement principle of the rail surface signal [10]

The system records longitudinal rail surface irregularities with a spatial sampling interval of 5 mm and covers a wavelength range from approximately 20 mm to 1000 mm. Owing to the chord-based measurement geometry, the recorded amplitudes are subject to wavelength-dependent distortion described by the system transfer function. This systematic effect is compensated prior to further analysis by frequency-domain deconvolution using the inverse transfer function provided for the measurement system. The resulting signal represents a corrected longitudinal rail surface profile and forms the basis for the subsequent time-series analysis of short-wave corrugation development [10].

2.2 Time series construction

Based on the processed rail surface measurement data, time series were constructed to analyze the temporal development of short-wave rail corrugation in curved track sections. The evaluation aims to visualize changes in the analyzed rail surface indicators over successive measurement runs and to identify corrugation growth trends between maintenance interventions. Measurement dates were converted into a continuous numerical time axis to ensure consistent chronological ordering of observations. Measurement data from successive runs were spatially assigned to the corresponding curved track sections using their mileage ranges. For each curve and measurement run, a representative value was derived over the full curve length and used to construct the corresponding time series. All analyses refer exclusively to the inner rail of each curve, as short-wave corrugation predominantly develops on this rail. For each extracted curve segment and measurement run, the root mean square (RMS) value was computed. This metric provides a robust scalar measure of the overall magnitude of longitudinal surface irregularities, as the chord-based measurement signal oscillates around zero.

2.3 Spectral analysis of dominant wavelength (0–300 mm)

To complement the regression-based evaluation, the rail surface signal was analyzed spectrally to determine the dominant corrugation wavelength. For each curve and measurement run, a Fast Fourier Transform (FFT) was applied to obtain the wavelength spectrum of the longitudinal rail profile. The analysis was restricted to wavelengths between 0 mm and 300 mm [4, 7]. Prior to peak identification, the spectrum was smoothed using a moving-average filter to reduce local noise while preserving the dominant wavelength position. The wavelength corresponding to the global maximum within this range was defined as the dominant corrugation wavelength. An example of the resulting wavelength spectra obtained within one measurement run is shown in figure 2. One curve exhibits a confined short-wavelength range with elevated spectral amplitudes around approximately 80–120 mm, indicating a pronounced and well-defined dominant corrugation wavelength. In contrast, the other curve shows only an isolated spectral outlier without a consistently developed peak structure, reflecting the absence of a clearly periodic surface irregularity.

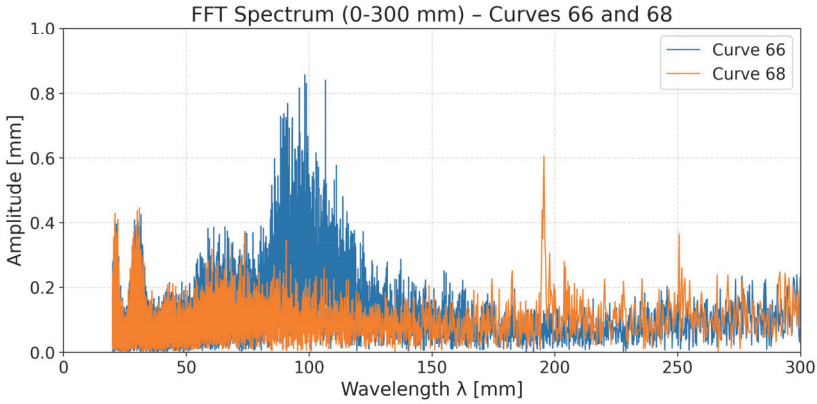

Figure 2 Comparison of FFT spectra from a curve with pronounced short-wave corrugation in blue and a curve with no corrugation in orange (range of 0–300 mm)

2.4 Regression analysis

The objective of the regression analysis is to quantify the temporal development of short-wave rail corrugation based on the derived rail surface indicators. Building on the time series described in the previous section, regression analyses were performed individually for each curve and running direction. The analysis focuses on indicators for which a systematic temporal increase associated with corrugation growth can be expected. The dominant corrugation wavelength was not evaluated using regression methods, as no consistent growth behavior over time was identified; it was therefore considered only in comparative analyses. To account for maintenance-related interventions and non-uniform development phases, a segmented linear regression approach was applied. Instead of describing the entire time series with a single regression line, individual regression segments were identified between maintenance events or phases of approximately steady development. Segment identification was based on the processed time-series data, supported by signal smoothing and outlier handling to reduce the influence of short-term fluctuations or isolated disturbances.

3 Results

For the presentation and comparison of results, the evaluated curves were grouped according to curvature severity and documented rail steel grade, allowing a consistent assessment of corrugation growth behavior across different geometric conditions and materials. The analysis distinguishes between standard rail steel R260 and the head-hardened grades R350HT and R400HT. For the analysis of the dominant wavelength, the data was only split into the three different radius classes.

3.1 Corrugation growth rates

The corrugation growth rates obtained for the three radius classes and rail steel grades are shown in figure 3. A clear dependence on curve radius is evident, with the highest growth rates occurring in the smallest radius class (R ‹ 250 m) and systematically decreasing values with increasing radius. In the smallest radius class (R ‹ 250 m), the number of available observations for R260 is insufficient for a robust assessment. A comparison is therefore limited to the head-hardened grades, where R350HT exhibits higher growth rates than R400HT, indicating inferior performance under severe curvature conditions. For the second radius class (250 m ‹ R ‹ 400 m), R350HT again shows higher median corrugation growth rates than R400HT. In this class, R260 performs slightly better than R350HT in terms of the median growth rate, but exhibits a noticeably larger scatter, pointing to less stable corrugation behavior. In the largest radius class (400 m ‹ R ‹ 600 m), the differences between the rail steel grades become small. This can be attributed to the reduced excitation of corrugation in large-radius curves, leading to generally lower corrugation growth and diminishing material-related effects.

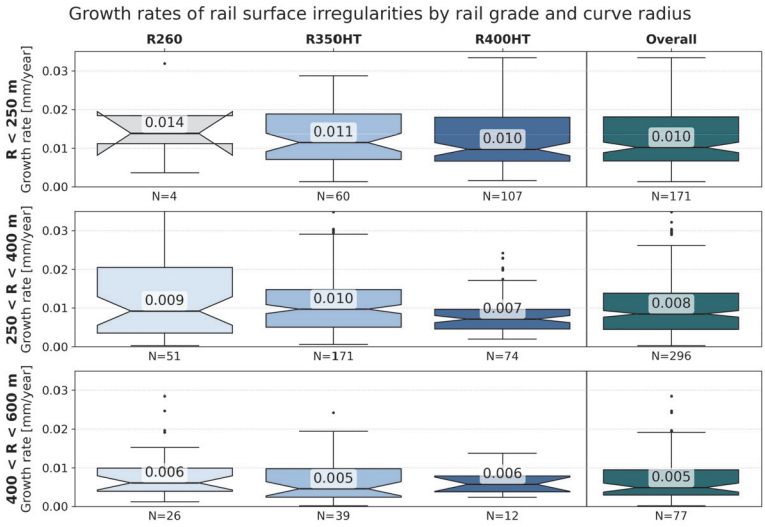

Figure 3 Corrugation growth rates derived from rail surface measurements, grouped by radius class and rail steel grade

3.2 Analysis of dominant corrugation wavelengths

In addition to the growth-rate analysis, dominant corrugation wavelengths were evaluated using spectral analysis of the rail surface measurements. For each curve and measurement run, the dominant wavelength within the range from 0 mm to 300 mm was identified and grouped by radius class (figure 4). In the smallest radius class (R ‹ 250 m), dominant wavelengths cluster in the range of approximately 75 to 100 mm, with a median of 90 mm. This value is close to one sixth of the sleeper spacing of 600 mm (= 100 mm), indicating a structural influence of sleeper support on wavelength selection. For intermediate radii (250 m ‹ R ‹ 400 m), the median dominant wavelength increases to approximately 120 mm, corresponding to one fifth of the sleeper spacing (= 120 mm). In the largest radius class, the median further increases to around 130 mm and the distribution becomes more diffuse, suggesting weaker wavelength fixation under reduced loading conditions. Overall, the results show that dominant corrugation wavelengths increase with curve radius and that discrete fractions of the sleeper spacing act as a governing structural parameter in the wavelength selection of short-wave corrugation.

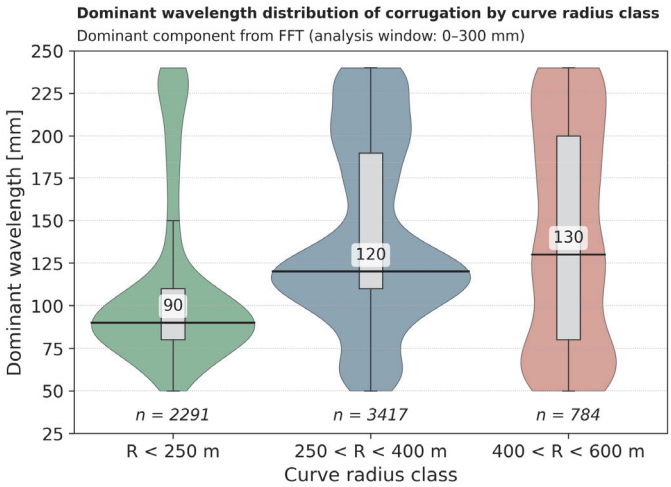

Figure 4 Dominant corrugation wavelengths grouped by radius class

4 Conclusion

The results demonstrate that short-wave rail corrugation and its temporal development can be reliably quantified using long-term rail surface measurements acquired under real operating conditions. The applied methodology, combining curve-specific time-series construction and segmented regression analysis, proved robust for identifying corrugation growth behavior on an individual curve basis. Corrugation growth is strongly governed by curve radius, with small-radius curves exhibiting consistently higher growth rates than larger radii, identifying curvature as the dominant influencing factor. Rail steel grade has a secondary but measurable influence on corrugation growth. Higher-strength steels generally exhibit lower growth rates and reduced scatter, with R400HT performing best; however, significant corrugation growth persists in small-radius curves even for high-strength rails, indicating that material improvements alone cannot compensate for unfavorable geometric and loading conditions.

The spectral analysis supports the physical plausibility of the findings, showing that dominant corrugation wavelengths increase with curve radius and cluster around discrete fractions of the sleeper spacing, indicating sleeper support characteristics as a governing structural parameter in wavelength selection.
The present evaluation is expressed as a function of time. As traffic volumes on the investigated line remained stable during the observation period, temporal growth can be regarded as proportional to accumulated load. Future investigations should additionally relate corrugation growth to accumulated gross tonnage in order to enable load-normalized comparison between lines with different traffic levels. Differentiation by sleeper type was not feasible due to the predominance of wooden sleepers; future work should therefore extend the analysis to lines with more balanced track structures and combine corrugation growth assessment with rail wear analysis to support geometry-dependent and material-specific maintenance strategies.

References

[1] Grassie, S.L., Kalousek, J.: Rail corrugation: characteristics, causes and treatments, Proceedings of the Institution of Mechanical Engineers, Part F: Journal of Rail and Rapid Transit, 207 (1993) 1, pp. 57–68

[2] Andersson, C., Johansson, A.: Prediction of rail corrugation generated by three-dimensional wheel–rail interaction, Wear, 257 (2004) 3–4, pp. 423–434

[3] Han, J., Xiao, X., Wu, Y., Wen, Z., Zhao, G.: Effect of rail corrugation on metro interior noise and its control, Applied Acoustics, 130 (2018), pp. 63–70

[4] British Standards Institution: Railway applications – Track – Acceptance of works – Part 5: Procedures for rail reprofiling in plain line, switches, crossings and expansion devices, BS EN 13231-5, 2018.

[5] Grassie, S.L.: Rail corrugation: characteristics, causes, and treatments, Proceedings of the Institution of Mechanical Engineers, Part F: Journal of Rail and Rapid Transit, 223 (2009) 6, pp. 581–596

[6] Wang, Z., Lei, Z., Zhu, J.: Study on the formation mechanism of rail corrugation in small radius curves of metro, Journal of Mechanical Science and Technology, 37 (2023) 9, pp. 4521–4532

[7] Auer, F.: Zur Verschleißreduktion von Gleisen in engen Bögen, Doctoral thesis, Graz University of Technology, Graz, 2010.

[8] Matsumoto, A., Sato, Y., Ono, H., Tanimoto, M., Oka, Y., Miyauchi, E.: Formation mechanism and countermeasures of rail corrugation on curved track, Wear, 253 (2002), pp. 178–184

[9] Loidolt, M., Marschnig, S.: Potenzial einer vorhandenen Datenquelle am Beispiel Schienenoberfläche, ZEV, 146 (2022) 10

[10] Loidolt, M.: Integration of short-wave effects into asset management of railway infrastructure: An alternative perspective on the quality behaviour of tracks, doctoral thesis, Graz University of Technology, Graz, 2024.